JOURNAL OF SOLID STATE CHEMISTRY 114, 129–137 (1995)

# Infrared, Polarized Raman, and SERS Spectra of Betaine Hydrogen Oxalate Monohydrate

Daizy Philip and G. Aruldhas[1]

*Department of Physics, University of Kerala, Kariavattom, Trivandrum 695 581, India*

Received October 12, 1993; in revised form March 9, 1994, accepted March 16, 1994

**Infrared and polarized Raman spectra of betaine hydrogen oxalate monohydrate are recorded and analyzed. The observed bands are assigned on the basis of vibrations due to oxalic acid, betaine, and water molecules. In the crystal it is found that oxalic acid molecules occupy a lower site and that betaine exists in zwitterionic form. Oxalic acid and water molecules are involved in strong hydrogen bonding. Band assignments are confirmed by deuteration. Surface enhanced Raman scattering (SERS) spectra recorded in two silver colloids reveal chemisorption through different adsorption sites. The observed SERS spectra are interpreted on the basis of different adsorption sites, geometries, and adsorbate conformation/orientation. The change of the SERS spectrum with time is due to the different stabilities of the adsorbed states. The oxalic acid molecules of the compound are likely to be in a tilted orientation with respect to the silver surface.** 

## INTRODUCTION

Betaine, $(CH_3)_3N^+CH_2COO^-$, forms adducts with many inorganic and organic molecules (1–4). Among them $(CH_3)_3NCH_2COO \cdot (COOH)_2 \cdot H_2O$, betaine hydrogen oxalate monohydrate (BHO), is unique as it does not show any high-temperature phase transitions (4). From IR spectroscopic investigations of bis (betaine) telluric acid (5) and betaine monohydrate (6), some of the internal modes of betaine have been identified. Detailed vibrational spectroscopic data for betaine and its derivatives and adducts have not yet been reported.

Surface enhanced Raman scattering (SERS) spectroscopy is a useful technique for the study of the physical and chemical adsorption of molecules onto metals. The vibrational assignment of molecules adsorbed onto metal surfaces is of importance when there exists a metal–molecule complex formation as in chemisorption. In such cases, orientation of the complex with respect to the metal surface is an important factor in determining the Raman scattering cross section of each fundamental vibration (7, 8). The metal–adsorbate interaction is evidenced by the presence of some bands in the 150–300 $cm^{-1}$ region that are assigned to its stretching vibrations (9–18), which depend on the nature of the adsorbed species. As BHO has $COO^-$ and $(COOH)_2$, its SERS studies, along with IR and Raman spectra, are expected to give interesting results.

[1] To whom correspondence should be addressed.

## EXPERIMENTAL

Polarized Raman spectra of a 2 × 3 × 4 mm single crystal of BHO have been recorded for the four orientations $z(YY)X$, $Z(YZ)X$, $Z(XY)X$, and $Z(XZ)X$ corresponding to the polarizability tensor components $\alpha_{yy}$, $\alpha_{yz}$, $\alpha_{xy}$, and $\alpha_{xz}$, respectively. Here, the $X$, $Y$, and $Z$ axes of observation coincide with the crystal axes $a$, $b$, and $c$. A Spex Ramalog 1401 double monochromator equipped with a Spectra Physics Model 165 $Ar^+$ laser (5145 Å, 80 mW) is used to record the spectra. FTIR spectra (4000–400 $cm^{-1}$) are obtained with a PE 7600 FTIR spectrometer with the sample in KBr. The IR spectra (4000–200 $cm^{-1}$) recorded on a PE 983 spectrometer with the sample in KBr and nujol are also used. Raman and IR spectra of the deuterated polycrystalline sample obtained by repeated recrystallizations from $D_2O$ are used to confirm the assignments.

The SERS spectra have been investigated in two different silver colloids: (i) A stable greenish-yellow silver colloid (hereafter called colloid 1) having a sharp absorption maximum at 400 nm prepared from sodium borohydride and silver nitrate by the method described by Creighton *et al.* (19); and (ii) a greenish-gray colloid (hereafter called colloid 2) with a broad adsorption band around 430 nm prepared from silver nitrate and sodium citrate (20). Chemicals required are from Sigma. Deionized water has been used throughout.

Absorption spectra of the silver colloids, BHO, and adsorbed BHO (Figs. 1 and 2) have been recorded on a UV-240 Shimadzu UV–visible recording spectrophotometer. When BHO gets adsorbed onto colloid 1, the color changes to light pink and the absorption band at 400 nm broadens and shifts to 405 nm. Further, an additional



0022-4596/95 $6.00

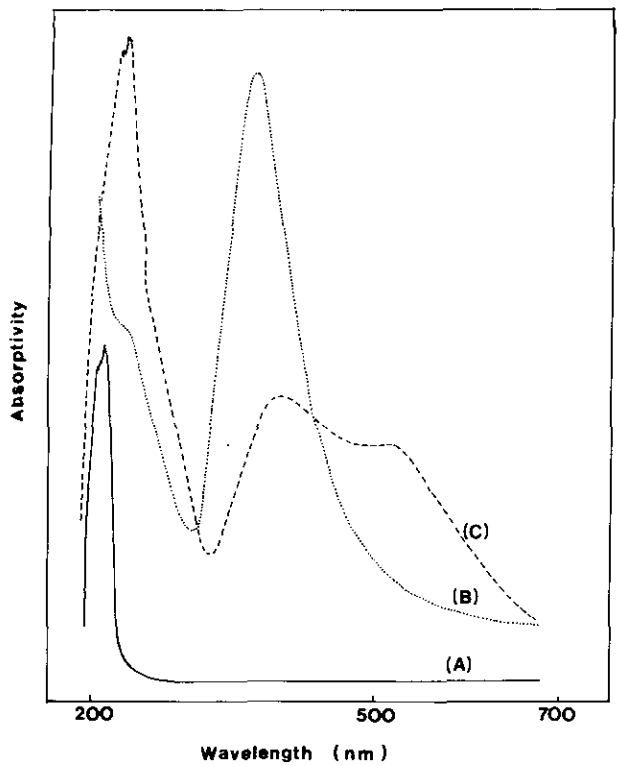


FIG. 1. Absorption spectrum of (A) BHO, (B) colloid 1, and (C) BHO adsorbed on colloid 1.

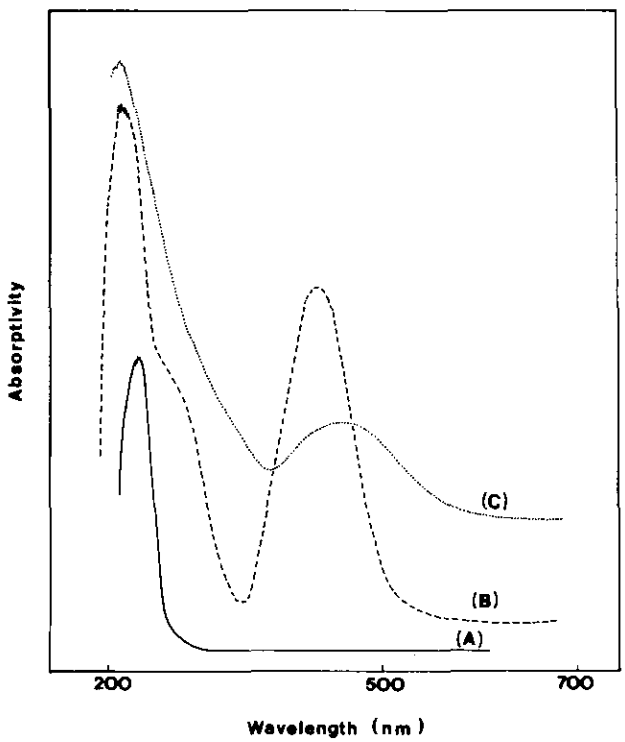


FIG. 2. Absorption spectrum of (A) BHO, (B) Colloid 2, and (C) BHO adsorbed on colloid 2.

very broad band appears around 530 nm. In the case of colloid 2, the color changes to gray and the broad band around 430 nm broadens with its center around 460 nm.

To record the SERS spectra, 1 ml of $10^{-3}$ $M/10^{-4}$ $M$ BHO solution was added to 60 ml of colloid 1. The resulting solution was placed in a rectangular quartz cell and the Raman spectra were recorded on a Dilor GMBH Z 24 spectrometer with 50 mW laser power. In the case of colloid 2, 1 ml of $10^{-3}$ $M/10^{-4}$ $M$ BHO solution was added to 20 ml of colloid 2. As BHO coagulated colloid 2 in about 1 h (when placed in the laser beam), the scanning of the spectrum was completed in about 30 min. This difficulty was not experienced in colloid 1, as it took about 3 hr to coagulate.

## RESULTS AND DISCUSSION

### *Infrared and Polarized Raman Spectra*

The planar oxalic acid molecule, $(COOH)_2$, is centrosymmetric (21) with 18 internal modes ($9A_g + 9A_u$). In the tetramolecular space group $C2/c$ of BHO (4), because $(COOH)_2$ occupies the general site $C_1$, inactive modes will become active and each of the Raman and IR active modes will be split into four components, one each in the $A_g$, $B_g$, $A_u$, and $B_u$ species of the factor group $C_{2h}$.

For $\nu$ C=O mode (C=O stretching), two Raman bands are observed (Table 1) in the $Z(YY)X$ orientation ($A_g$ species). The polarized band (Fig. 3) at 1736 $cm^{-1}$ probably arises from the Raman-active $\nu_2$ mode and the other one from the Raman-inactive $\nu_{11}$. (For an explanation of $\nu_1, \nu_2, \ldots, \nu_{18}$, see the footnote to Table 1.) In IR, three bands are observed for the $\nu$ C = 0 mode. The maximum number expected in the spectrum of the polycrystalline sample is four. Without the lower site symmetry effect, one would have obtained only two bands in IR. The observation of the three bands clearly shows that at least one component is from the infrared inactive $\nu_2$ mode. Similar arguments hold for the $\nu_7$ and $\nu_{17}$ modes. All the internal modes of $(COOH)_2$ could not be assigned independently, as bands due to betaine complicate the spectrum.

It is well known that the deprotonated carboxylic group ($COO^-$) has two very characteristic absorption bands around 1410 and 1600 $cm^{-1}$ which are respectively the symmetric and asymmetric stretching modes. For a COOH group, $\nu_{as}$ C = 0 is expected around 1720 and $\nu_s$ C = 0 around 1260 $cm^{-1}$ (22). In the IR spectrum of pure betaine (Table 1) the very strong band at 1630 $cm^{-1}$ with a shoulder at 1610 $cm^{-1}$ and the bands in the region 1400–1500 $cm^{-1}$ indicate the presence of a deprotonated carboxylic group, in agreement with the zwitterionic structure suggested by Leifer and Lippincott (23). In BHO, since $COO^-$, $(COOH)_2$, and water molecules are present,

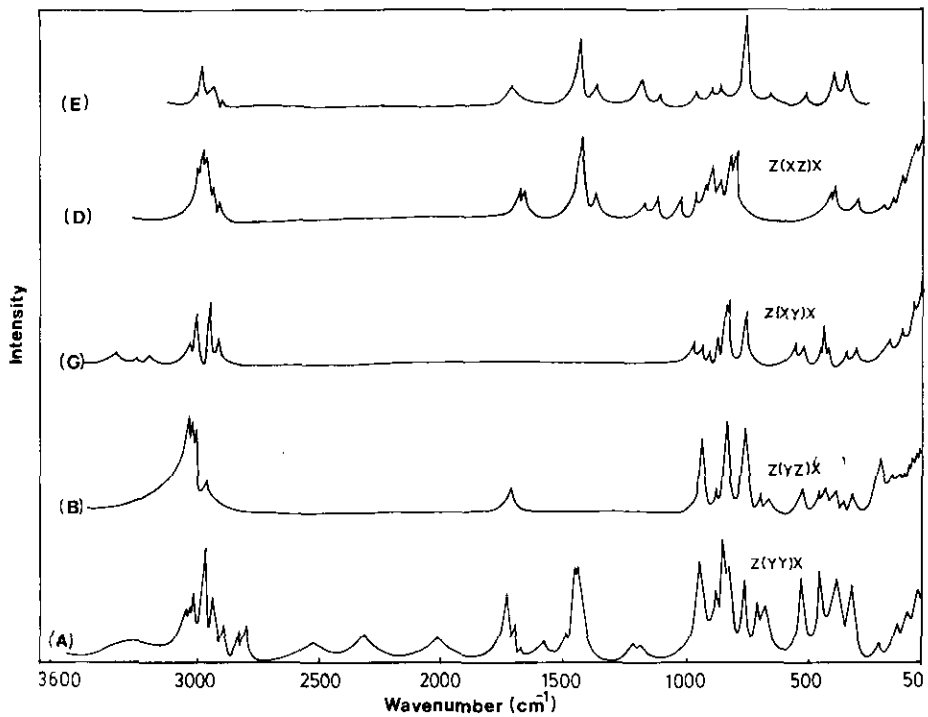


FIG. 3. Raman spectrum of (A, B, C, and D) BHO single crystal and (E) deuterated BHO.

it is difficult to identify the band due to the $\nu_{as}COO^-$ of betaine in the 1500–1700 $cm^{-1}$ region. However, it is reasonable to assume that betaine exists as a zwitterion in BHO since the three IR bands observed at 1645, 1620, and 1550 cannot be due to the bending mode of $H_2O$ alone. Further, the band at 1620 $cm^{-1}$ does not show considerable change on deuteration. Also, this frequency is close to the band observed for $\nu_{as}COO^-$ in pure betaine (Table 1). Therefore, the IR band at 1620 $cm^{-1}$ in BHO is possibly due to the $\nu_{as}COO^-$ of the betaine molecule in it.

On deuteration, the band around 1400 $cm^{-1}$ in both Raman and IR spectra shows a decrease in intensity, and an additional medium broad band appears around 1090 $cm^{-1}$ in IR. Therefore, it is reasonable to assume that the band at 1400 $cm^{-1}$ in BHO has some contribution from the O–H bond which may be due to the O–H $\cdots$ O deformation of the strongly hydrogen-bonded water molecule (24). The strong IR bands (Fig. 4) observed at 720 and 670 $cm^{-1}$ are assigned to $\nu_{15}$ ($\delta COO^-$) and the librational modes of water. In the deuterated spectrum (IR), the intensities of these bands are reduced slightly and two additional weak bands appear at 685 and 615 $cm^{-1}$. This confirms the assignment of the librational modes of water, which is again indicative of the involvement of the water molecule in hydrogen bonding. The trio of bands in the 1900–2600 $cm^{-1}$ region (22) arises from the very strong hydrogen bond between different oxalic acid molecules.

The Raman bands in the region 3000–3080 $cm^{-1}$ are not polarized, whereas those in the 2900–3000 $cm^{-1}$ are polarized. Hence, the assignment of the former to $\nu_{as}CH_3$ and of the latter of $\nu_sCH_3$ is justifiable. The stretching modes of $CH_2$ overlapped those of $CH_3$. When a $CH_2$ or $CH_3$ group is attached to a nitrogen atom, the stretching modes shift to low frequencies (22, 25). Therefore, the strong IR band appearing at 2840 $cm^{-1}$ and the weak Raman bands in the 2800–2900 $cm^{-1}$ region are also assigned to the (N)C–H stretching mode. The symmetric and asymmetric bending modes of the $CH_3$ group usually occur around 1375 and 1460 $cm^{-1}$ (22, 25). The bending mode of $CH_2$ is also expected around 1460 $cm^{-1}$. Independent assignment of these modes could not be made, as the bands due to $(COOH)_2$ and $COO^-$ also appear in this region.

### *SERS Spectra in Silver Colloids*

SERS spectra (Fig. 5) recorded in both colloids show a low-frequency band between 160 and 240 $cm^{-1}$ which is not seen in the Raman spectrum of the aqueous solution of BHO. It is also seen that the spectra are different in the two colloids at different concentrations of the adsorbate. These features may be interpreted as follows.

It is reported that the frequency of the metal–molecule stretching mode increases with decrease in molecular mass (14). As the silver–molecule stretching frequency is

TABLE 1
Vibrational Spectral Data ($cm^{-1}$) and Band Assignments

| BHO | | | | | | | | Betaine | | |
|---|---|---|---|---|---|---|---|---|---|---|
| Raman | | | | | | IR | | | | |
| $z(yy)x$ | $z(yz)x$ | $z(xy)x$ | $z(xz)x$ | Powder | Deuterated | Hydrated | Deuterated | Raman | IR | Assignments |
| | | 3360vw | | 3375sh | | | | | | |
| 3350–3200vwbr | | 3280vw<br>3225vw | | 3303mbr<br>3225sh | | 3350sbr | | | | $\nu_{as}$ and $\nu_s H_2O$ |
| 3050m | 3050s | 3055w | 3038m | 3040s | 3050w | 3030m | | 3077vw | | |
| | | | | | | | 3019m | | | $\nu_{as}CH_3$, $\nu_1$, and $\nu_{10}$ |
| 3042m | 3042s | | 3028s | 3032s | 3029m | 3000m | | 3047w | | |
| | | 3036m | | | | | | | | |
| 3032s | 3028s | | 3000m | | | | | 3026m | 3020s | |
| | | | | | | | | 3014s | | |
| | | | | | | | | 2978m | | |
| 2973vs | | 2970m | 2974w | 2980vs | 2974mbr | | 2980brsh | | | |
| | 2975w | | | | | 2900m | | 2963vs | 2980m | $\nu_s CH_3$ |
| 2938m | | 2940w | 2940vw | 2944s | 2940w | | 2935m | | | |
| | | | | | | | | 2936m | | |
| 2900w | | | | | | | | | | |
| | | | | | | | | 2880vwbr | | |
| 2828w | | | | 2836vw | | | | | | $\nu$(N)C–H |
| | | | | | | 2840s | 2810sbr | 2800vwbr | | |
| 2800w | | | | 2811w | | | | | | |
| 2530wbr | | | | | | 2500m | 2465m | | | Triobands, |
| 2370wbr | | | | 2500vw | | 2370m | | | 2240mbr | combinations, and |
| | | | | | | | 2130m | | | $\nu D_2O$ |
| 2015wbr | | | | | | 1970mbr | | | | |
| 1736m | | | | 1748w | | 1735s | 1720vs | | | |
| | 1733w | | 1710w | 1727m | 1755mbr | 1720m | | | | $\nu_2$ and $\nu_{11}$ |
| | | | | | | | 1700sh | | | |
| 1707w | | | | 1720m | | 1700w | | | | |
| 1670w | | | | | | 1645s | 1685m | | 1630vs | $\delta H_2O$ and |
| | | | 1695w | | | 1620s | 1615s | | 1610sh | $\nu_{as}COO^-$ |
| 1570wbr | | | | | | | | | | |
| | | | | | | 1550w | 1530sh | | | |
| 1484w | | | | | | | | | 1490m | $\delta_{as}CH_3$, $\delta CH_2$, |
| 1458s | | | 1460s | 1463s | | 1480m | 1460m | | 1470m | $\nu_s COO^-$, and $\nu_3$ |
| | | | | | 1470s | | | | | |
| 1452s | | | 1406w | 1440sh | | 1460vw | 1435w | 1460s | 1450w | |
| | | | | | | 1430m | 1410m | | 1410m | |
| | | | | | | | 1090mbr | | | |
| | | | | 1396m | | 1400s | 1385s | 1330m | 1390m | $\delta$O–H ··· O, |
| | | | | | | | | | | $\delta$O–D ··· O, |
| | | | | | 1400w | | | | | |
| | | | | 1350vw | | 1330w | 1320w | 1320w | 1330s | $\delta_s CH_3$ and $\nu_{12}$ |
| | | | | | | | 1310w | | 1230m | |
| 1220wbr | | | | | | 1280m | 1260m | | | |
| | | | 1213w | 1224w | 1222mbr | | | | | |
| 1190wbr | | | | | | 1250m | 1230m | | | $\nu_4$ and $\delta D_2O$ |
| | | | | | | | 1210m | | | |
| | | | | 1153vw | | 1190vs | 1175s | | 1130w | |
| | | | 1148w | | | | | | | |
| | | | | 1140vw | 1143w | 1125m | 1115m | | | $\nu$C–N and $\nu_{13}$ |
| | | | 1005w | | | | | | 1010w | |
| | | | | 1010w | | 1020m | 1010w | | | |
| | | | | 1005m | | | | | | |
| | | | | | | | 980s | | | |
| | | 993w | 993w | | | 990s | | 975w | 980m | $\gamma CH_3$ |
| | | | | | 998w | | 935w | | | |
| | | 955w | 957w | 965vw | | 950w | | 952w | 950m | |

TABLE 1—*Continued*

| BHO | | | | | | | | Betaine | | |
|---|---|---|---|---|---|---|---|---|---|---|
| Raman | | | | | | IR | | | | |
| $z(yy)x$ | $z(yz)x$ | $z(xy)x$ | $z(xz)x$ | Powder | Deuterated | Hydrated | Deuterated | Raman | IR | Assignments |
| 953s | 952s | | | | | | | | | |
| | | 928vw | | 939m | 938w | 930s | 915s | 940w | 930m | $\gamma CH_2$ |
| | | | 928m | | | | | | | |
| 886m | 887w | 889w | 890w | 900vw | | 880s | | | | |
| | | | | | 899w | | 865s | | | |
| 860vs | | 855m | | 868s | | 835m | | 894w | 890s | $\nu_5$, $\nu_6$, and $\nu_{14}$ |
| | 855s | | 857m | | | | 835w | | | |
| 845s | | 850m | | 860sh | | 800m | | | | |
| | | | | | | | 820s | | | |
| | | | | | | | | | 750m | |
| 773s | 778s | 778m | 778m | 791vs | 789vs | 780m | | 780s | | $\nu_7$ |
| | | | | | | | | | 730s | |
| | | | | 732w | | | 710s | | | |
| 718m | 716vw | | | | 696wbr | 720s | | | | |
| | | | | 700vw | | | 685w | | | $RH_2O$ and $\nu_{15}$ |
| 684m | 682vw | | | | | | 660m | | | |
| | | | | | | 670s | 615wbr | | | |
| | | | | | | | | | 590s | |
| | | 578w | | | | | | | | |
| | | | | | | 585w | 495mbr | 540w | 520m | |
| 540s | 540w | | | 553w | 552w | | | | | $\nu_8$ and $\nu_{16}$ |
| | | 546w | | | | | | | | |
| | | | | | | 500s | | | | |
| | | | | | | | | | 440w | |
| | 469w | 473w | | 458w | | 450m | 440wbr | 453w | | |
| 469s | | | 446w | | 439m | | | | 385w | |
| | 447w | 468m | | | | | | | | $\nu_9$ and $\delta NCC$ |
| | | | | 425W | 391m | 385w | | | | |
| | 400w | 445w | 425w | | | | | | | |
| 398sbr | | | | 380w | | | | | | |
| | 370w | 370w | | | | | | | | |
| | | | | | | 365w | | | 360s | |
| 337s | 338w | 336w | 334w | | | | 350m | | | |
| | | | | 290w | | 310w | | | 290w | $\nu_{17}$ |
| 220vw | 225m | | 228w | | | | | | | |
| | | | | | | 295w | 315wbr | 361w | 260s | |
| | | | | | | 240m | | | | |
| | | | | | | 215m | | | | |
| | 178vwbr | 188w | 188w | | | | | | | |
| | | | | 187w | | | | 169wbr | | $\nu_{18}$, $TH_2O$, and |
| | 150wbr | 140w | 151w | | | | | | | other external modes |
| 145vw | | | | 79m | | | | 90s | | |
| | 118w | | 147w | | | | | | | |
| 95wbr | | | | | 78m | | | 83s | | |
| | 95m | 95s | 95s | 41m | | | | | | |
| | | | | | | | | 62s | | |
| | 85m | | | | | | | | | |
| 54s | | | 56s | | | | | | | |
| | 71m | 70s | | | | | | | | |
| | 56w | | | | | | | | | |

*Note.* vs, very strong; s, strong; m, medium; w, weak; vw, very weak; br, broad; sh, shoulder; $\nu_s$, summetric stretch; $\nu_{as}$, asymmetric stretch; $\delta$, bend; R, libration; T, translation; $\gamma$, rocking. $\nu_1(A_g) = \nu OH$, $\nu_2(A_g) = \nu C = 0$, $\nu_3(A_g) = \nu C{-}O$, $\nu_4(A_g) = \delta OH$, $\nu_5(A_g) = \gamma C{=}O$, $\nu_6(A_g) = \nu C{-}C$, $\nu_7(A_g) = \gamma OH$, $\nu_8(A_g) = \rho COO$, $\nu_9(A_g) = \delta COO$, $\nu_{10}(A_u) = \nu_{OH}$, $\nu_{11}(A_u) = \nu C{=}O$, $\nu_{12}(A_u) = \delta OH$, $\nu_{13}(A_u) = \nu C{-}O$, $\nu_{14}(A_u) = \gamma OH$, $\nu_{15}(A_u) = \delta COO$, $\mu_{16}(A_u) = \gamma C{=}O$, $\nu_{17}(A_u) = \rho COO$, $\nu_{18}(A_u) = \tau C{-}C$.

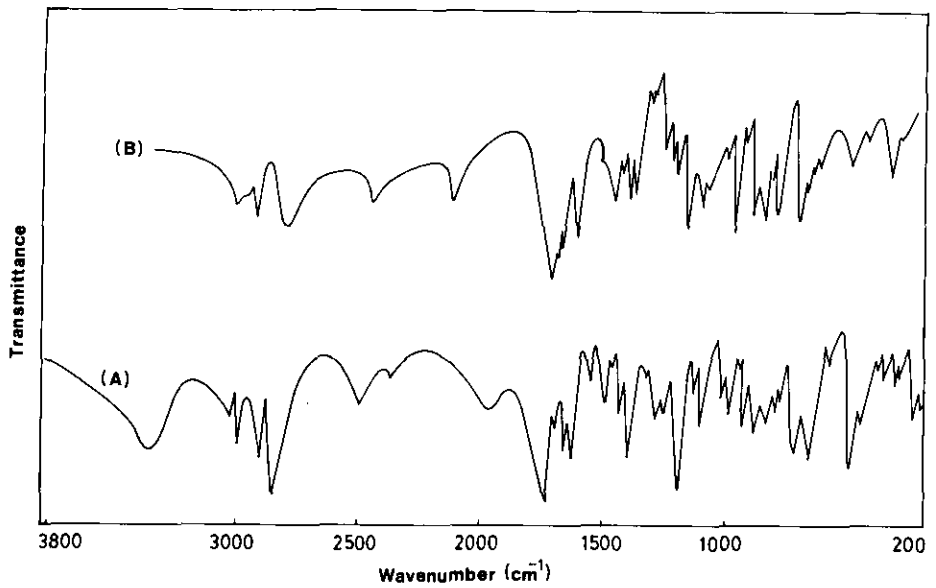


FIG. 4. IR spectrum of (A) BHO and (B) deuterated BHO.

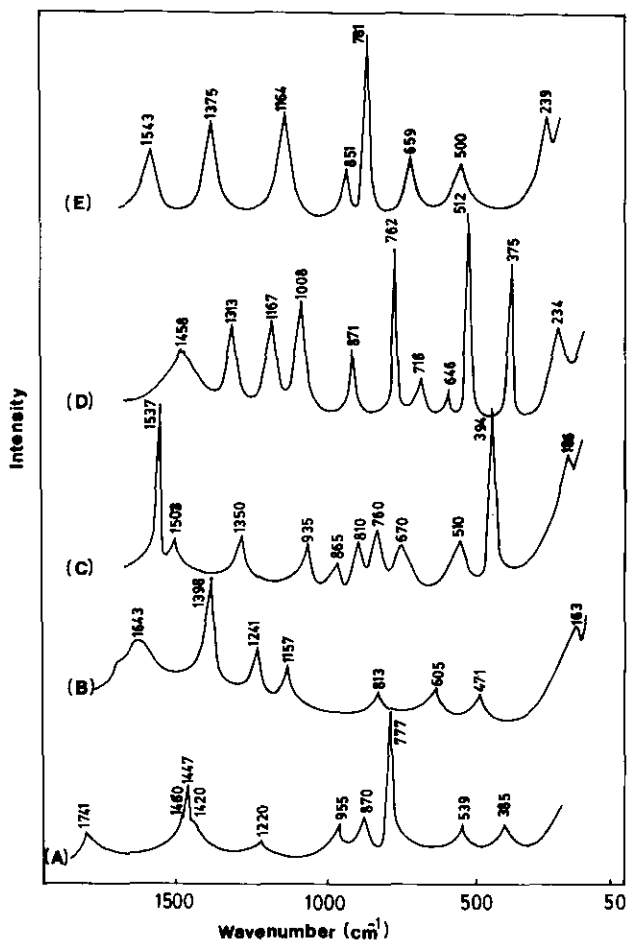


FIG. 5. (A) Raman spectrum of saturated aqueous solution of BHO; SERS spectrum of (B) BHO ($10^{-3}$ *M*) in colloid 1; (C) BHO ($10^{-4}$ *M*) in colloid 1; (D) BHO ($10^{-3}$ *M*) in colloid 2; and, (E) BHO ($10^{-4}$ *M*) in colloid 2.

163 $cm^{-1}$ in colloid 1 ($10^{-3}$ *M*) and 234 $cm^{-1}$ in colloid 2 ($10^{-3}$ *M*), it is possible that the silver surface is close to the betaine molecule in colloid 1 and to the oxalic acid molecule in colloid 2. These low-frequency bands correspond to the $\nu$ Ag–O modes of the silver–adsorbate chemisorbed system (9–18), and the adsorption occurs through the carboxylic groups in betaine and oxalic acid molecules present in BHO. The differences observed in the SERS spectra recorded in the two colloids are therefore justifiable. The conclusion that in colloid 2 the oxalic acid molecule is close to the silver surface is further supported by the presence of the low-frequency band around 245 $cm^{-1}$ in the SERS spectrum of pure oxalic acid (Fig. 6).

The frequency shift of the SERS bands with concentration is probably due to changes in the adsorbate conformation/orientation (10, 16, 17). Some of the possible adsorption geometries are shown in Fig. 7. In colloid 1, as betaine is close to the silver surface, the geometries A, B, and C are predominant; in colloid 2, D, E, F, G, and H predominate. Assignment of the observed SERS bands (Table 2) has been made on the basis of literature data (9, 14, 16, 28, 29) for molecules with similar functional groups. The acidic configuration (A) in Fig. 7 is possible at the expense of a proton from oxalic acid. The band at 1643 $cm^{-1}$ at $10^{-3}$ *M* concentration in colloid 1 may be due to this configuration (10). At $10^{-4}$ *M* this band disappears and two new bands appear at 1503 and 1537 $cm^{-1}$ (Fig. 5). These may arise from the monodentate and bidentate configurations [10, 15] shown in Figs. 7B and 7C. In colloid 2, the band at 1458 $cm^{-1}$ ($10^{-3}$ *M*) corresponds to $\delta_{as}CH_3$ and the bond at 1543 $cm^{-1}$ to $\nu_s COO^-$. The presence of these bands shows that the betaine molecule

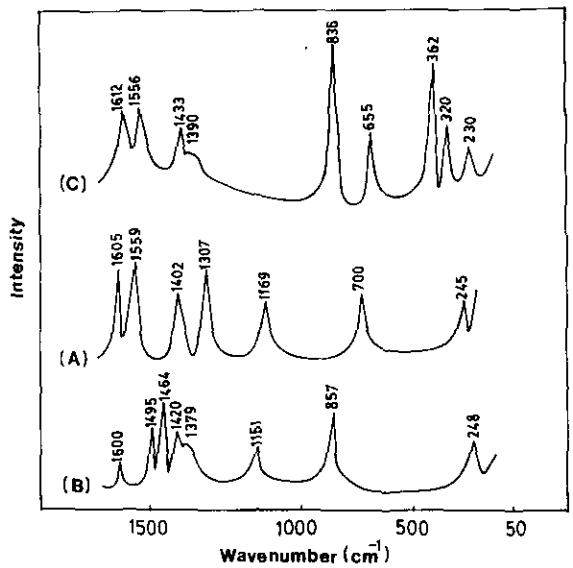


FIG. 6. SERS spectrum of (A) oxalic acid in colloid 1, (B) oxalic acid in colloid 2, and (C) BHO ($10^{-4}$ *M*) 1 hr after mixing with colloid 2.

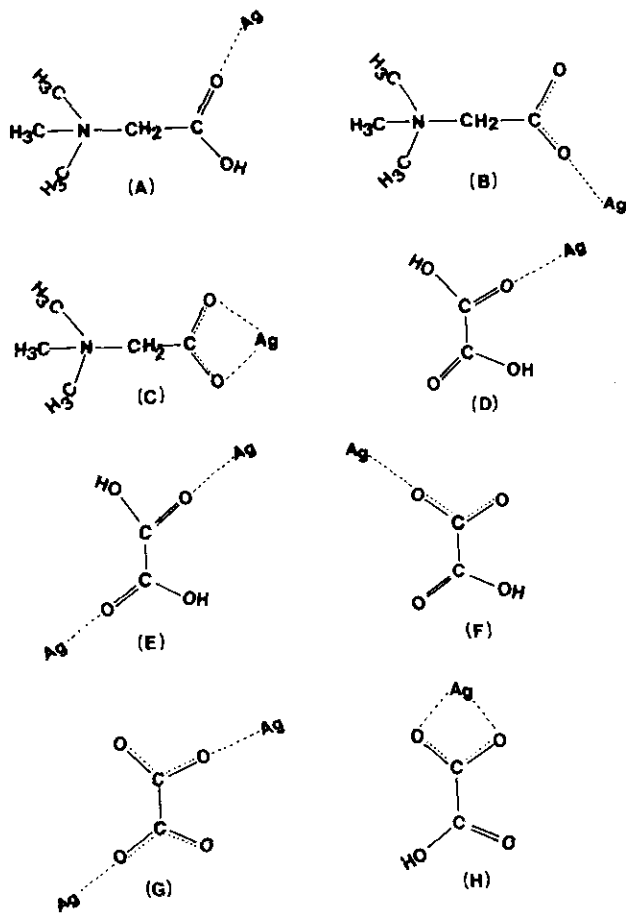


FIG. 7. Schematic representation of some of the adsorption geometries of BHO (A, B, and C) in colloid 1 and (D, E, F, G, and H) in colloid 2.

TABLE 2
SERS Spectral Data ($cm^{-1}$) and Band Assignments of BHO

| Saturated solution of BHO | SERS spectrum in colloid 1 | | SERS spectrum in colloid 2 | | Assignments |
|---|---|---|---|---|---|
| | $10^{-3}$ *M* | $10^{-4}$ *M* | $10^{-3}$ *M* | $10^{-4}$ *M* | |
| 1741 | | | | | $\nu_{as}COOH$ |
| | 1643 | | | | $\nu_{as}COO^-$ |
| 1460 | | 1537 | | | |
| 1447 | | 1503 | 1458 | 1543 | $\delta_{as}CH_3$ and $\nu_sCOO^-$ |
| 1420 | | | | | |
| | 1398 | | | | δOH, |
| | | | | 1375 | |
| 1220 | 1241 | 1350 | 1313 | | |
| | | | | 1164 | $\delta_sCH_3$ and νC–N |
| | 1157 | | 1167 | | |
| | | | 1008 | | |
| 955 | | 935 | | | $\gamma CH_3$ and $\gamma CH_2$ |
| 870 | | 865 | 871 | 851 | νC–C |
| | 813 | 810 | 762 | | |
| | | | | 781 | |
| 777 | | 760 | 718 | | $\gamma_gOH$ |
| | 605 | | | 659 | |
| | | 670 | 646 | | |
| 539 | 471 | 510 | 512 | 500 | $\rho COO^-$ |
| 385 | | 394 | 375 | | $\delta_gCOO^-$, δNCC |
| | 163 | 186 | 234 | 239 | $\nu_{Ag}$–O |

is also near the silver surface. Interesting changes have been noted in the SERS spectrum (Fig. 6) of BHO ($10^{-4}$ *M*) in colloid 2 recorded 1 hr after mixing. The bands around 1543 and 1375 $cm^{-1}$ show doubling and the most intense band at 781 $cm^{-1}$ is replaced by a band at 835 $cm^{-1}$. Further, two additional strong bands appear at 362 and 320 $cm^{-1}$. This is because of the different stabilities (10) of the multiple adsorbed states given in Fig. 7D to 7H. That is, even at the same concentration of the adsorbate, another adsorbed state becomes predominant after some time (10, 17). The splitting of the band at 1543 $cm^{-1}$ into two bands at 1612 and 1556 $cm^{-1}$ may be due to a change in configuration from bidentate (Fig. 7H) to monodentate (Fig. 7F) and acidic (Fig. 7D) configuration (10, 15). The intensity of the band at 835 $cm^{-1}$ corresponding to the C–C stretching mode increases substantially after 1 hr. This may be due to the photochemical decomposition (26) of BHO leading to the formation of graphite at the silver surface or to the presence of multiple adsorbed states already discussed.

In addition to the adsorbed states shown in Fig. 7, it is possible that another adsorbed state involving a $CH_3$ group is present, as observed in the case of 5-methyl cytosine (16). The proximity of the $CH_3$ group to the silver surface may form silver–betaine complexation

TABLE 3
SERS Spectral Data ($cm^{-1}$) and Band Assignments of Oxalic Acid

| Oxalic acid in colloid 1 | Oxalic acid in colloid 2 | Assignments |
|---|---|---|
| 1605 | 1600 | $\nu_2$ and $\nu_{11}$ |
| 1559 | 1495 | |
| | | $\nu_3$ |
| | 1464 | |
| 1402 | | |
| | 1420 | |
| 1307 | 1379 | $\nu_{12}$, $\nu_4$, and $\nu_{13}$ |
| 1169 | | |
| | 1151 | |
| 700 | 857 | $\nu$C–C |
| 245 | 248 | $\nu$Ag–O |

which anchors the molecules on the silver surface. The appearance of the band at 935 $cm^{-1}$ in colloid 1 at $10^{-4}$ *M* concentration which corresponds to the rocking mode of $CH_3$ is indicative of such an adsorbed state [16]. The shift of the $\nu A_g$–O band with concentration is also due to the presence of different adsorption geometries (27).

According to the surface selection rule (30), the vibrational modes involving atoms that are close to the metal surface are enhanced more when compared with other vibrations. Therefore, one expects bands due to betaine to be enhanced in colloid 1 and those due to oxalic acid to be enhanced in colloid 2. A comparison of the SERS spectral data (Tables 2 and 3) shows that bands due to both betaine and oxalic acid are enhanced in colloid 2, indicating the nearness of the betaine molecule to the silver surface. In the SERS spectrum of pure oxalic acid (Fig. 6) the band due to the OH in-plane bending mode ($\delta$OH) is enhanced (Table 3). It may then be inferred that pure oxalic acid assumes a perpendicular orientation with respect to the silver surface (30). In BHO, as bands due to both $\gamma$ OH (OH out-of-plane bending) and $\delta$OH are enhanced (Table 2), the oxalic acid molecule is in a tilted rather than a flat or a perpendicular orientation with respect to the silver surface (30).

## CONCLUSION

In the crystal, oxalic acid molecules occupy a lower site. Strong hydrogen bonding between oxalic acid molecules is evident from the existence of triobands. The observation of the $\delta$OH $\cdots$ O mode at 1400 $cm^{-1}$ and the librational modes of water at 720 and 670 $cm^{-1}$ in the IR spectra indicate strong hydrogen bonding of the water molecules. BHO has different adsorption sites. The silver surface is close to the betaine molecule in colloid 1 and to the oxalic acid molecule in colloid 2. In both colloids multiple adsorbed states are present. The change of the SERS spectrum with time is due to the different stabilities of the multiple adsorbed states. The intensity enhancement of the bands due to both the in-plane and the out-of-plane OH bending modes of the oxalic acid molecules is indicative of a tilted orientation with respect to the silver surface.

## ACKNOWLEDGMENTS

D. P. thanks the CSIR, New Delhi for a research associateship. The authors are grateful to Professor S. Haussühl, Institute of Crystallography, University of Cologne, Germany for providing the single crystals used in the investigation. Help received from Professor R. Kaleysa Raj of the Department of Biochemistry and Dr. T. S. Anirudhan, Department of Chemistry, University of Kerala is acknowledged.

## REFERENCES

1. W. Shildkamp and J. Spilker, *Z. Krystallogr.* **168,** 159 (1984).
2. W. Shildkamp, G. Schafer, and J. Spiler, *Z. Kristallogr.* **168,** 187 (1984).
3. O. Freitag, H. J. Bruckner, and H. G. Unruh, *Z. Phys. B* **61,** 75 (1985).
4. S. Haussühl and Wang Jiang, *Z. Kristallogr.* **187,** 249 (1989).
5. M. M. Ilczyszyn, T. Lis, J. Baran, and H. Ratajczak, *J. Mol. Struct.* **265,** 293 (1992).
6. K. M. Harmon and G. F. Avci, *J. Mol. Struct.* **117,** 295 (1984).
7. R. Aroca and R. E. Clavijo, *Spectrochim. Acta Part A* **44,** 171 (1988).
8. U. K. Sarkar, S. Chakrabarti, T. N. Misra, and A. J. Pal, *Chem. Phys. Lett.* **200,** 55 (1992).
9. R. E. Clavijo, B. Mutus, R. Aroca, J. R. Dimmock, and O. A. Philips, *J. Raman Spectrosc.* **19,** 541 (1988).
10. Sun Kai, Wan Chaozhi, and Xu Guangzhi, *J. Raman Spectrosc.* **20,** 267 (1989).
11. Wan Chaozhi, He Tianjing, Gao Xiaoping, Li Jungquing, Xin Houwen, and Liu Fan Chen, *J. Mol. Struct.*, **140,** 227 (1986).
12. M. Pagannone, B. Fornari , and G. Mattei, *Spectrochim. Acta. Part A* **43,** 621 (1987).
13. P. Hildebrandt, R. S. Czernuszewicz, C. A. Grygon, and T. G. Spiro, *J. Raman Spectrosc.* **20,** 645 (1989).
14. G. D. Chumanov, R. G. Efremov, and I. R. Nnbiev, *J. Raman Spectrosc.* **21,** 43 (1990).
15. Sun Kai, Wan Chaozhi, and Xu Guangzhi, *Spectrochim. Acta. Part A* **45,** 1029 (1989).
16. S. Sanchez-Cortes and J. V. Gracia-Ramos, *J. Raman Spectrosc.* **23,** 61 (1992).
17. W. S. OH, S. W. Sun, and M. S. Kun, *J. Raman Spectrosc.* **19,** 261 (1988).
18. L. F. C. De Olieveira, P. S. Santos, and J. C. Rubin, *J. Raman Spectrosc.* **22,** 197 (1991).
19. J. A. Creighton, C. G. Blatchford, and M. G. Albrecht, *J. Chem. Soc. Faraday Trans. 2* **75,** 790 (1979).
20. P. C. Lee and D. Meisel, *J. Phys. Chem.* **86,** 3391 (1982).
21. J. De Villepin, A. Novak, and D. Bougeard, *Chem. Phys.* **73,** 291 (1982).
22. C. N. R. Rao, "Chemical Applications of Infrared Spectroscopy." Academic Press, New York, 1963.
23. A. Leifer and E. R. Lippincott, *J. Chem. Soc.* **79,** 5098 (1957).

24. S. N. Vinogradov and R. H. Linnel, "Hydrogen Bonding," Van Nostrand, New York, 1970.
25. L. J. Bellamy, "Infrared Spectra of Complex Molecules," Vol. 2. Chapman and Hall, London, 1975.
26. J. S. Suh, M. Moskovits, and J. Shakhsemampour, *J. Phys. Chem.* **97,** 1678 (1993).
27. H. Lee, S. W. Suh, and M. S. Kim, *J. Raman Spectrosc.* **21,** 237 (1990).
28. S. Aruan and G. Shanmugan, *J. Raman Spectrosc.* **16,** 229 (1985).
29. S. Sanchez-Cortes and J. V. Gracia-Ramos, *J. Raman Spectrosc.* **21,** 679 (1990).
30. M. Moskovits, *Rev. Mod. Phys.* **57,** 783 (1985).